Acta Oceanol. Sin., 2023, Vol. 42, No. 3, P. 76–88
https://doi.org/10.1007/s13131-022-2128-8
http://www.aosocean.com
E-mail: ocean2@hyxb.org.cn

Origin of hydrocarbon fluids and discussion of abnormal carbon isotopic compositions in the Lishui-Jiaojiang Sag, East China Sea Shelf Basin

Jingqi Xu*

Shanghai Branch of China National Offshore Oil Corporation (CNOOC) Co., Ltd., Shanghai 200335, China

Received 7 May 2022; accepted 21 October 2022

Abstract

The hydrocarbon gases in the L1 gas field of the Lishui-Jiaojiang Sag have been commonly interpreted to be an accumulation of pure sapropelic-type thermogenic gas. In this study, chemical components, stable isotopic compositions, and light hydrocarbons were utilized to shed light on the origins of the hydrocarbon fluids in the L1 gas pool. The hydrocarbon fluids in the L1 gas pool are proposed to be a mixture of three unique components: mid-maturity oil from the middle Paleocene coastal marine Lingfeng source rock, oil-associated (late oil window) gas generated from the lower Paleocene lacustrine Yueguifeng source rock, and primary microbial gas from the paralic deposits of the upper Paleocene Mingyuefeng source rock. Here, for the first time, the hydrocarbon gases in the L1 gas pool are diagnosed as mixed oil-associated sapropelic-type gas and microbial gas via four pieces of principal evidence: (1) The abnormal carbon isotopic distributions of all methane homologues from C_1 (CH_4 or methane) to C_5 (C_5H_{12} or pentane) shown in the Chung plot; (2) the diagnostic ^{13}C-depleted C_1 compared with the thermogenic sapropelic-type gas model, while $\delta^{13}C_2$ (C_2H_6 or ethane) and $\delta^{13}C_3$ (C_3H_8 or propane) both fit perfectly; (3) the excellent agreement of the calculated carbon isotopic compositions of the pure thermogenic gas with the results of the thermal simulated gas from the type-II_1 kerogen-rich Yueguifeng source rock; and (4) the oil-associated gas inferred from various binary genetic diagrams with an abnormally elevated gas oil ratio. Overall, the natural gases of the L1 gas pool were quantified in this study to comprise approximately 13% microbial gas, nearly 48% oil-associated sapropelic-type gas, and 39% of nonhydrocarbon gas. The microbial gas is interpreted to have been codeposited and entrained in the humic-kerogen-rich Mingyuefeng Formation under favorable low-temperature conditions during the late Paleocene-middle Eocene. The microbial gas subsequently leaked into the structurally and stratigraphically complex L1 trap with oil-associated sapropelic-type gas from the Yueguifeng source rock during the late Eocene–Oligocene uplifting event. A small amount of humic-kerogen-generated oil in the L1 gas pool is most likely to be derived from the underlying Lingfeng source rock. The detailed geological and geochemical considerations of source rocks are discussed to explain the accumulation history of hydrocarbon fluids in the L1 gas pool. This paper, therefore, represents an effort to increase the awareness of the pitfalls of various genetic diagrams, and an integrated geochemical and geological approach is required for hydrocarbon-source correlation.

Key words: origin of hydrocarbons, carbon isotope, hydrogen isotope, light hydrocarbon, East China Sea Shelf Basin, Lishui-Jiaojiang Sag

Citation: Xu Jingqi. 2023. Origin of hydrocarbon fluids and discussion of abnormal carbon isotopic compositions in the Lishui-Jiaojiang Sag, East China Sea Shelf Basin. Acta Oceanologica Sinica, 42(3): 76–88, doi: 10.1007/s13131-022-2128-8

1 Introduction

Studies on the origins of the hydrocarbon fluids have significant implications for exploration strategies, although they remain challenging, as the complexity may exist due to the uncertainty of source rocks, migration, charging, mixing, and degradation. Exploration in the Lishui-Jiaojiang Sag of the East China Sea Shelf Basin (ECSSB) has been carried out for approximately 40 years, and only one gas field (i.e., L1 gas field) and ten oil- and gas-bearing structures have been discovered as of the end of 2021. The L1 gas field was discovered in 1997 and the first production began in 2015. The L1 gas field mainly produces hydrocarbon fluids from the upper Paleocene Mingyuefeng reservoirs. Oils and gases are also hosted in the lower-middle Paleocene rocks and basement in the Lishui-Jiaojiang Sag. Exploration in the Lishui-Jiaojiang Sag that targets the analogs of the L1 gas field has always been underway, but no commercial discovery has been achieved since then. One of the major challenges is the lack of understanding of the Paleocene petroleum system due to following reasons: (1) small hydrocarbon datasets due to few discoveries, limitations on fluid sampling techniques, and fluid contaminations; (2) geochemical records of hydrocarbon fluids obscured by the proliferous CO_2 influx accompanied with active volcanic activities; and (3) limited knowledge revealed about the deeply buried presumably excellent source rocks beneath the L1 gas field.

Over the past decades, many attempts have been made to

Foundation item: The "Seven Year Action Plan" East China Sea Special Project of CNOOC under contract No. CNOOC-KJ 135 ZDXM 39 SH02.

*Corresponding author, E-mail: xujq15@cnooc.com.cn

analyze the geochemistry of the hydrocarbon fluids in the L1 gas pool to deduce their origins (Table 1; Sun and Xi, 2003; Chen et al., 2008, Ge et al., 2012; Su et al., 2014; Li et al., 2019, 2021). Geochemical characterization of the source rocks, specifically, the organic enrichment, thermal maturities, organic types, and hydrocarbon generation potentials of Yueguifeng, Lingfeng, and Mingyuefeng formations, have been performed (Sun and Xi, 2003; Chen et al., 2008; Su et al., 2014; Li et al., 2019, 2021). There exists a consensus that Yueguifeng and Lingfeng formations are two principal effective source rocks for the discovered hydrocarbon fluids in the Lishui-Jiaojiang Sag. Excellent source rocks in the Yueguifeng Formation (high original TOC and hydrogen index values) penetrated by a couple of wells suggest that they are rich in sapropelic kerogens and were deposited in a lacustrine environment. However, none of the wells have encountered the Yueguifeng source rocks beneath the L1 gas field region. The shallow-marine Lingfeng source rocks are humic-kerogen-rich and show a poorer source rock quality. Biomarkers, carbon stable isotopes, and major gas chemical compositions have been used to constrain the origin, thermal maturity, and accumulation history of the L1 gas field (Sun and Xi, 2003; Chen et al., 2008; Ge et al., 2012; Su et al., 2014; Li et al., 2021). Most of those studies have concluded a predominant thermogenic sapropelic-type gas from the Yueguifeng Formation by using genetic diagrams of $CH_4/(C_2H_6+C_3H_8)$ vs. $\delta^{13}CH_4$ (Bernard et al., 1976; Whiticar, 1999) and $\delta^{13}CH_4$ vs. $\delta^{13}C_2H_6$ and $\delta^{13}C_3H_8$ (Dai et al., 2014). In terms of the oil from the L1 gas field, various interpretations, mainly mixing models, have been proposed (see Table 1). The lack of hydrocarbon fluids and possible source rock variability in different sags/subsags have made it difficult to ascertain the origin of oil in the L1 gas field. All previous studies have reached an agreement on the inorganic source of the ^{13}C enriched CO_2 gas in the L1 gas field (Sun and Xi, 2003; Chen et al., 2008; Su et al., 2014; Huang et al., 2020; Li et al., 2021).

It is worth mentioning that none of the previous studies on the L1 gas pool have performed stable hydrogen isotope analyses, which have been suggested to provide critical clues for gas interpretation (Schoell, 1983; Chung et al., 1988; Berner and Faber, 1996; Whiticar, 1999, 2020; Dai et al., 2014; Wang et al., 2015; Milkov and Etiope, 2018; Liu et al., 2019). Moreover, a few genetic diagrams used for gas interpretations have been suggested for revision by a new approach with a more robust dataset (e.g., Milkov and Etiope, 2018; Milkov, 2021). The objective of this study is to reinvestigate the genetic characteristics of the L1 gas field and hopefully provides an innovative perspective on the hydrocarbon accumulations in the Lishui-Jiaojiang Sag. Herein, we report a suite of geochemical data of the oil and gas in the L1 gas field to summarize their origins and genetically related properties. In particular, carbon and hydrogen isotope analyses and a series of recently proposed genetic diagrams were applied to establish the hydrocarbon accumulation model of the L1 gas pool.

2 Geological background

The Lishui-Jiaojiang Sag is located in the southwestern part of the East China Sea Shelf Basin, which is a NNE–SSW extending backarc rift basin within the convergence zone between the Eurasian, Pacific, and Philippine Sea Plates (Fig. 1a; Schellart and Lister, 2005; Cukur et al., 2011). The Lishui-Jiaojiang Sag covers approximately 2.0×10^4 km^2 and is subdivided into four NE–SW trending structural regions: the western Lishui Subsag, the Lingfeng Ridge, the eastern Lishui Subsag, and the Jiaojiang Sag (Fig. 1b). The tectonic framework of the Lishui-Jiaojiang Sag, a series of half-graben or graben features along NNE- and NE-striking faults, is a consequence of the late Cretaceous–middle Eocene rifting events caused by the northwest-dipping subduction induced slab rollback of the Pacific Plate beneath the Eurasian Plate (Figs 1b and c; Yang et al., 2004; Schellart and Lister, 2005; Cukur et al., 2011; Liang and Wang, 2019). The geochronological studies of the Paleocene succession suggest that the clastic flux was predominantly from Mesozoic volcanic rocks, volcaniclastic rocks, and granite from the Zhemin Uplift to the west with a minor contribution from the Yandang Uplift to the east (Figs 1a and b; e.g., Li et al., 2016). The Lishui-Jiaojiang Sag underwent a significant erosional event prior to the Miocene deposition related to a major phase of exhumation in a basinwide compressional regime during the late Eocene-Oligocene (Figs 1c and 2).

The stratigraphic units, overlying the residual basement in the Lishui-Jiaojiang Sag, are grouped into three main sequences: syn-rift (upper Cretaceous–middle Paleocene), post-rift (upper Paleocene–middle Eocene), and thermal subsidence (Neogene–Quaternary) (Fig. 2). The recognized petroleum systems in the Lishui-Jiaojiang Sag are principally focused on the Paleocene strata, which is also the focus of this paper (Fig. 2). The Paleocene interval is thickest to the east in each subsag and progressively thins toward the western margins (Fig. 1c). The Paleocene succession consists of three distinct units, namely, the Yueguifeng, Lingfeng, and Mingyuefeng formations in ascending order (Fig. 2). The deposition of the Yueguifeng Formation may have taken place in a lacustrine setting during the transition from rifting initiation to rifting climax. It largely consists of dark gray mudstones and thin layers of siltstones. The overlying Lingfeng Formation, which accumulated during the rifting climax, is characterized by coastal marine argillaceous deposition. The sand-

Table 1. Selected published studies investigating the origins of hydrocarbon fluids in the L1 gas pool

Study	Sample	Interpreted origin
Sun and Xi (2003)	gas	mixture of mid- to high-maturity sapropelic-type gas from the Yueguifeng Formation and low- to mid-maturity humic-type gas from the Lingfeng Formation
	oil	from the Lingfeng and Mingyuefeng formations
Chen et al. (2008)	gas	mid-maturity sapropelic-type gas from the Yueguifeng Formation
Ge et al. (2012)	oil	from the Lingfeng and Mingyuefeng formations
Su et al. (2014)	gas	mixture of high-maturity sapropelic-type gas from the Yueguifeng Formation and the low maturity humic-type gas from the Mingyuefeng Formation
	oil	predominantly low-maturity humic-type oil from the Mingyuefeng Formation
Li et al. (2021)	gas	predominantly oil-associated gas from the Yueguifeng Formation
	oil	predominantly from the Lingfeng Formation with a minor portion from the Yueguifeng Formation
This study	gas	mixture of primary microbial methane from the Mingyuefeng Formation and mid-maturity sapropelic-type gas from the Yueguifeng Formation
	oil	early- to mid-maturity humic-type oil from the Lingfeng Formation

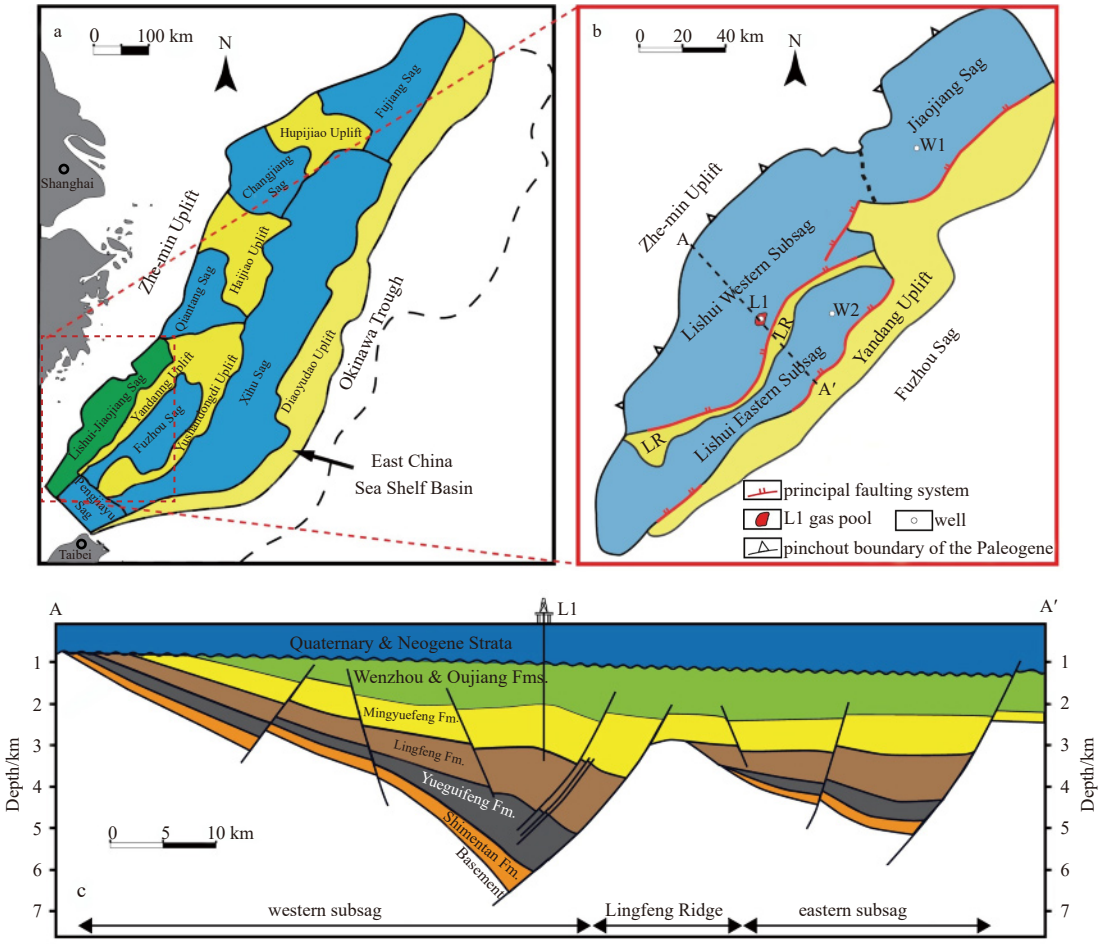

Fig. 1. Schematic map showing the location of the Lishui-Jiaojiang Sag (a), major geological structures, L1 gas field, and selected wells in the Lishui-Jiaojiang Sag (b), and geological units and faulting systems in a schematic cross-section (c). Location of c is shown as A–A′ in b. Fm., Formation; LR, Lingfeng Ridge.

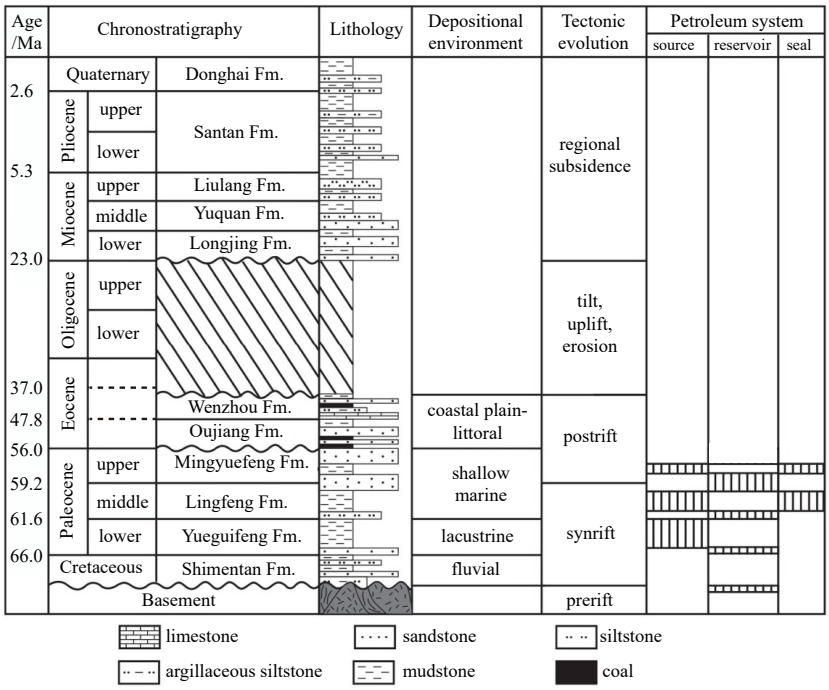

Fig. 2. Generalized stratigraphic column, tectonic evolution, and petroleum system of the Lishui-Jiaojiang Sag. Note the thickness of each unit is not to scale. Fm., Formation.

stone-rich Mingyuefeng Formation, unconformably overlying the Lingfeng Formation, records a complete cycle of marine transgression and regression during the early postrift stage. The L1 gas field is located at the anticline under a series of northwest-dipping normal faulting regimes in the Western Subsag (Figs 1b and c). The hydrocarbon pay zone is located between approximately 2 185 m and 2 285 m true vertical depth subsea (TVDSS) in a structural and stratigraphical complex of the upper Paleocene Mingyuefeng reservoirs (Fig. 1c). There exists a consensus that the Yueguifeng and Lingfeng formations are two principal effective source rocks in the Lishui-Jiaojiang Sag, while the Mingyuefeng Formation is relatively too shallow to reach the oil window (Fig. 2). The Yueguifeng source rocks, penetrated by few wells in the Eastern Subsag and Jiaojiang Sag, are relatively sapropelic kerogen (Type II kerogen)-rich and demonstrate the best source rock quality, with the highest TOC of ~4% and hydrogen index (HI) of ~350 mg/g (Chen et al., 2008; Li et al., 2019). Nevertheless, the Yueguifeng source rock in the Western Subsag is least well understood with few wells reached, particularly on the east side (paleo-depocenter) of the Western Subsag. The Lingfeng source rocks, characterized by abundant humic kerogens (Type III kerogens), have much poorer qualities with the highest TOC of ~2.5% and HI of ~200 mg/g compared to the Yueguifeng source rocks (Chen et al., 2008; Li et al., 2019).

3 Material and methods

In this paper, five well-head fluid samples were collected from the L1 gas pool using stainless steel bottles for analyses of chemical compositions, stable carbon and hydrogen isotopic compositions, and light hydrocarbons. Geochemical records of two duplicate hydrocarbon samples from one drill stem test (DST) analysis of the pay zone tested in the discovery Well L1 were also compiled. The stable hydrogen isotopes of methane were analyzed by a ThermoFisher Scientific Delta V Advantage mass spectrometer. Gas components were separated on an HP-PLOT Q column (27.5 m×0.32 mm×0.45 μm) with helium as the carrier gas (2 mL/min). The gas chromatograph oven temperature was initially 40℃ for 3 minutes, then was increased to 200℃ at 50℃/min and held at 200℃ for 5 minutes. Stable isotope ratios for hydrogen are reported in δ notation in per mil (‰) relative to VSMOW. The stable carbon isotope ratios of gas components were measured by an Elementar IsoPrime 100 mass spectrometer with an Agilent 7890B gas chromatograph. Each gas component, separated by using a gas chromatograph, was converted into CO_2 in a combustion interface and then finally measured by a mass spectrometer. The stable isotope results are reported as $\delta^{13}C$ relative to VPDB in per mil (‰). Gas chemical composition analyses were performed on an Agilent 6890N gas chromatograph equipped with a flame ionization detector and a thermal conductivity detector. The saturate-aromatic-resin-asphaltene (SARA) separation was achieved by asphaltene precipitation in hexane and then liquid chromatographic fractionation of the oil into saturate, aromatic and resin fractions. To obtain light-hydrocarbon fingerprints, the oil samples were analyzed using a gas chromatograph (Agilent, 7890B) equipped with a flame ionization detector and an HP-PONA fused silica capillary column (50 m×0.20 mm×0.50 μm). The components were collected with a liquid nitrogen cold trap for 5 min, and the eluting hydrocarbons were detected using a flame ionization detector (FID) at a temperature of 310℃. The initial oven temperature was maintained at 40℃ for 10 min, then ramped up to 70℃ at a rate of 4℃/min and then to 300℃ at a rate of 8℃/min. The final temperature was maintained for 30 minutes. The vitrinite reflectance analyses of the Well L1 were carried out by the Laboratory of Exploration and Development Research Institute, China offshore Naihai west corporation.

4 Result

4.1 *Molecular compositions of natural gases*

The molecular compositions of the gas samples from the L1 gas pool are listed in Table 2. The major nonhydrocarbon gases in the L1 gas pool are CO_2 and N_2, accounting for average values of 35.05% and 2.86% respectively. Methane, the principal component of hydrocarbon gas in the L1 gas pool, ranges from 51.83% to 56.55%. Ethane and propane account for average portions of 3.59% and 1.98% respectively. The wet gas signature is reflected by the average dryness value of 0.89 ($C_1/\Sigma(C_1–C_5)$) according to the classification scheme by Schoell (1980).

4.2 *Carbon and hydrogen isotopes of natural gases*

The stable carbon and hydrogen isotopic compositions of the natural gases from the L1 gas pool are listed in Table 3. The average stable carbon isotopes of C_1, C_2, and C_3 are –46.54‰, –29.95‰, and –27.36‰ respectively. The average $\delta^{13}C$ value of CO_2 is –6.28‰. The methane hydrogen isotope composition is –174.79‰ on average.

4.3 *Bulk geochemical parameters of condensate oil*

The average bulk density and sulfur content of the L1 oil samples are 0.753 g/cm^3 and 0.008 4%, respectively (Table 4). The SARA compositions of the L1 oil samples are shown in Table 4 with average 89.58% saturates, 9.63% aromatics, 0.63% resins, and 0.16% asphaltenes.

4.4 *Light hydrocarbons of condensate oil*

Representative gasoline-range chromatograms are shown in Fig. 3. The geochemical parameters of the light hydrocarbons in the condensate oil samples are listed in Table 5. Among methyl cyclohexane (MCH), *n*-heptane (*n*-C_7), and dimethyl cyclo-

Table 2. Molecular compositions and gas ratios of natural gases from the L1 gas pool

Well	Formation	Chemical composition (volume)/%									Gas ratio		Data source
		C_1	C_2	C_3	*i*-C_4	*n*-C_4	*i*-C_5	*n*-C_5	CO_2	N_2	$C_1/\Sigma(C_1–C_5)$	$C_1/(C_2+C_3)$	
Production wells	MYF	56.55	3.74	2.11	0.50	0.64	0.26	0.19	32.86	3.09	0.88	9.66	this paper
	MYF	54.45	3.59	2.03	0.48	0.62	0.25	0.19	35.70	2.64	0.88	9.70	
	MYF	51.83	3.40	1.92	0.45	0.59	0.24	0.18	38.44	2.91	0.88	9.75	
	MYF	54.60	3.67	2.09	0.49	0.64	0.26	0.19	34.73	3.28	0.88	9.48	
	MYF	51.97	3.40	1.91	0.45	0.58	0.24	0.17	38.27	2.94	0.88	9.78	
Discovery well	MYF	55.45	3.63	1.88	0.42	0.47	0.15	0.09	34.15	3.55	0.89	10.06	DST
	MYF	55.10	3.67	1.92	0.43	0.48	0.16	0.09	34.50	3.44	0.89	9.86	

Note: MYF, Mingyuefeng; DST, drill stem test.

Table 3. Stable carbon and deuterium isotopes of natural gases from the L1 gas pool

Well	Formation	C isotope/‰								H isotope/‰	Data source
		C_1	C_2	C_3	i-C_4	n-C_4	i-C_5	n-C_5	CO_2	C_1	
Production wells	MYF	–46.87	–30.29	–27.59	–28.42	–26.67	–26.61	–26.30	–6.92	–173.80	this paper
	MYF	–46.73	–30.24	–27.59	–28.34	–26.67	–26.42	–26.20	–6.88	–173.11	
	MYF	–46.58	–30.15	–27.56	–28.44	–26.42	–26.67	–26.01	–6.77	–177.00	
	MYF	–46.58	–30.11	–27.44	–28.36	–26.63	–26.25	–25.83	–7.10	–175.06	
	MYF	–46.62	–30.01	–27.34	–28.15	–26.86	–26.05	–26.37	–6.62	–174.98	
Discovery well	MYF	–46.30	–29.55	–26.96	–	–26.86	–	–	–5.03	–	DST
	MYF	–46.13	–29.31	–27.07	–	–26.93	–	–	–4.67	–	

Table 4. Bulk compositional and physical characteristics of oil samples from the L1 gas pool

Well	Formation	Density/(g·cm^{-3})	S content/%	SARA				Data source
				SAT/%	ARO/%	NSO/%	ASP/%	
Production wells	MYF	0.752	0.006 3	87.9	11.4	0.5	0.2	this paper
	MYF	0.753	0.006 3	88.8	10.7	0.4	0.1	
	MYF	0.761	0.008 1	88.2	11.0	0.6	0.2	
	MYF	0.754	0.006 3	87.4	11.9	0.6	0.1	
	MYF	0.752	0.005 8	88.1	11.1	0.6	0.2	
Discovery well	MYF	0.751	0.013 0	95.5	3.9	0.5	0.1	DST
	MYF	0.751	0.013 0	91.2	7.4	1.2	0.2	

Note: SAT, saturated hydrocarbons; ARO, aromatic hydrocarbons; NSO, resins; ASP, asphaltenes.

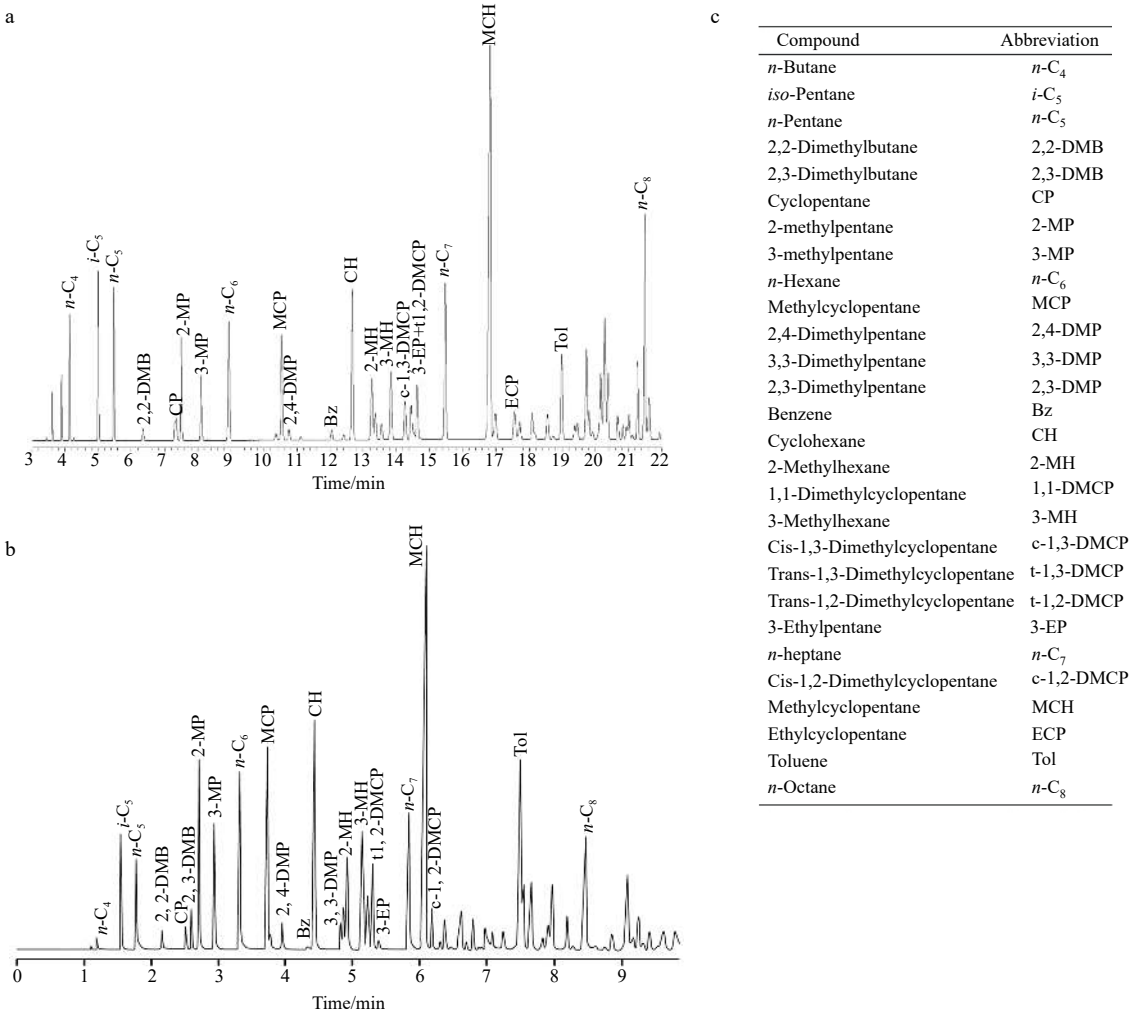

c

Compound	Abbreviation
n-Butane	n-C_4
iso-Pentane	i-C_5
n-Pentane	n-C_5
2,2-Dimethylbutane	2,2-DMB
2,3-Dimethylbutane	2,3-DMB
Cyclopentane	CP
2-methylpentane	2-MP
3-methylpentane	3-MP
n-Hexane	n-C_6
Methylcyclopentane	MCP
2,4-Dimethylpentane	2,4-DMP
3,3-Dimethylpentane	3,3-DMP
2,3-Dimethylpentane	2,3-DMP
Benzene	Bz
Cyclohexane	CH
2-Methylhexane	2-MH
1,1-Dimethylcyclopentane	1,1-DMCP
3-Methylhexane	3-MH
Cis-1,3-Dimethylcyclopentane	c-1,3-DMCP
Trans-1,3-Dimethylcyclopentane	t-1,3-DMCP
Trans-1,2-Dimethylcyclopentane	t-1,2-DMCP
3-Ethylpentane	3-EP
n-heptane	n-C_7
Cis-1,2-Dimethylcyclopentane	c-1,2-DMCP
Methylcyclopentane	MCH
Ethylcyclopentane	ECP
Toluene	Tol
n-Octane	n-C_8

Fig. 3. Representative partial whole oil chromatograms of the oil samples from the L1 gas pool. a. Production well; b. DST sample from the discovery well; and c. typical compounds identified.

pentane (DMCP), MCH dominates the C_7 light hydrocarbons with an average value of 60.46%. And the average relative contents of *n*-C_7 and DMCP are 20.11% and 19.43%, respectively. The average values of light-hydrocarbon parameters of *n*-heptane value, *iso*-heptane value, paraffinicity, and aromaticity are 14.40, 1.26, 0.33, and 0.42, respectively.

5 Discussion

5.1 *Genetic types and thermal maturity of the hydrocarbon gases in the L1 gas pool*

The molecular composition (CH_4–C_5H_{12}) and stable carbon and hydrogen isotopes ($\delta^{13}C$ and δD) have been widely used to distinguish gases from various source rocks and thermal maturities (e.g., Schoell, 1983; Chung et al., 1988; Berner and Faber, 1996; Whiticar, 1999, 2020; Vandré et al., 2007; Dai et al., 2014; Wang et al., 2015; Milkov and Etiope, 2018; Liu et al., 2019; Milkov, 2021). One of the commonly used classification schemes differentiates "humic/coal-type" gas and "sapropelic/oil-type" gas by using ^{13}C-C_2H_6: "humic/coal-type" gas displays more positive $\delta^{13}C_2$ values than –28.5‰, while natural gas with $\delta^{13}C_2 \leqslant$ –28.5‰ is classified as "sapropelic/oil-type" gas (Dai et al., 2014; Liu et al., 2019). Together with the diagram of $\delta^{13}C_1$ vs. $\delta^{13}C_2$ and $\delta^{13}C_3$ (Fig. 4a), a sapropelic-type gas has been suggested for the hydrocarbon gas in the L1 gas pool in the previous studies. Moreover, according to the binary diagram of $C_1/(C_2+C_3)$ vs. $\delta^{13}C_1$ (Fig. 4b), a low- to mid-maturity thermogenic gas has been proposed. These evidences are the chief rationales for the interpretation of a low- to mid- maturity sapropelic-type gas in all previous studies (Sun and Xi, 2003; Chen et al., 2008; Su et al., 2014; Li et al., 2021). None of those previous studies have inferred the contribution of microbial methane to the L1 gas pool, as the typical microbial gas is characterized by ^{12}C-enriched methane ($\delta^{13}C$<–50‰) with a dryness index of $C_1/\Sigma(C_1–C_5) \geqslant 95\%$ according to Schoell (1980). In fact, there have been a few studies reporting that the boundaries between thermogenic gases and mixed gases depicted in the $C_1/(C_2+C_3)$ vs. $\delta^{13}C_1$ diagram are not explicit as the possible mixing of microbial gases cannot be completely ruled out (Whiticar, 1999; Vandré et al., 2007; Liu et al., 2019; Cesar et al., 2020; Milkov, 2021). Care should also be taken when using the $\delta^{13}C_1$-$\delta^{13}C_2$-$\delta^{13}C_3$ diagram and the $\delta^{13}C_2$ threshold of 28.5‰ to distinguish genetic types of hydrocarbon gas, as they are proven to be not globally applicable (Milkov, 2021). Therefore, attempts to adopt a few recently developed models proposed by Milkov and Etiope (2018), Whiticar (2020), and Milkov (2021) were made in this study to decipher the genetic types of the hydrocarbon gases from the L1 gas pool in the Lishui-Jiaojiang Sag.

As shown in Fig. 5, the $C_1/(C_2+C_3)$ vs. $\delta^{13}C_1$ diagram illustrates either an oil-associated thermogenic gas or a secondary microbial gas for the gas samples from the L1 gas pool, while the $\delta^{13}C_1$ vs. $\delta^{13}CO_2$ diagram indicates the nature of the oil-associated thermogenic gas. Secondary microbial gas is the product of petroleum biodegradation, commonly associated with clearly biodegraded oil and gas and characterized by $\delta^{13}CO_2$>2‰ (Milkov and Etiope, 2018). The gas chromatography analyses of

Table 5. Light hydrocarbon parameters of the oil samples from the L1 gas pool

Well	Formation	C_7/%			*iso*-heptane value	*n*-heptane value	Paraffinicity	Aromaticity	2, 4-DMP/ 2, 3-DMP	Data source
		n-C_7	MCH	ΣDMCP						
Production wells	MYF	20.46	60.27	19.27	1.00	14.99	0.34	0.49	0.42	this paper
	MYF	20.32	60.45	19.24	0.98	14.92	0.34	0.50	0.42	
	MYF	19.95	61.24	18.81	0.97	14.80	0.33	0.50	0.41	
	MYF	20.34	60.24	19.42	0.99	14.89	0.34	0.50	0.42	
	MYF	20.44	60.01	19.56	0.99	14.88	0.34	0.51	0.43	
Discovery well	MYF	20.52	59.73	19.75	2.00	13.59	0.34	0.39	–	DST
	MYF	18.71	61.28	20.00	1.92	12.76	0.31	0.04	–	

Note: *n*-C_7%=*n*-C_7×100/(*n*-C_7+MCH+ΣDMCP); MCH%=MCH×100/(*n*-C_7+MCH+ΣDMCP); ΣDMCP%=ΣDMCP×100/(*n*-C_7+MCH+ΣDMCP). *iso*-heptane value=(2-MH+3-MH)/(t-1, 2-DMCP+c-1, 3-DMCP+t-1, 3-DMCP); *n*-heptane value=(100×*n*-C_7)/(CH+2-MH+1,1-DMCP+3-MH+c-1,3-DMCP+t-1,3-DMCP+t-1,2-DMCP+*n*-C_7+MCH); paraffinicity=*n*-heptane/methylcyclohexane; aromaticity=toluene/*n*-heptane.

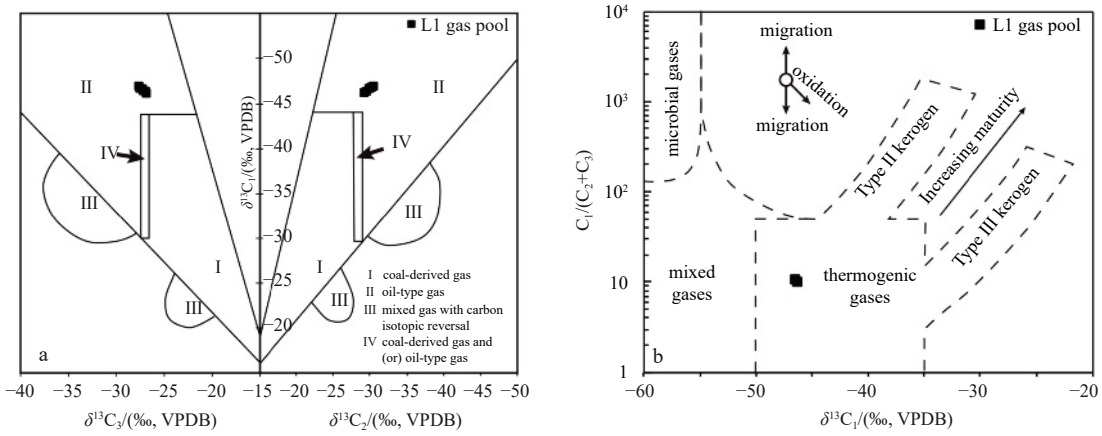

Fig. 4. Natural gases from the L1 gas pool plotted on the two most commonly used diagrams in all previous studies for gas interpretations. a. Plot of the $\delta^{13}C_1$ vs. $\delta^{13}C_2$ and $\delta^{13}C_3$ diagram (modified after Dai et al., 2014); b. plot of the $C_1/(C_2+C_3)$ vs. $\delta^{13}C_1$ diagram (modified after Bernard et al., 1976; Whiticar, 1999).

the light hydrocarbons of the condensate oil from the L1 gas pool show a full spectrum of typical ranges of C_4 to C_7 fractions (Fig. 3). The abundant saturated hydrocarbons, *n*-alkanes in particular, which are preferentially consumed during microbial activities, suggest that no major biodegradation has occurred (Fig. 3, Table 4). Thus, an oil-associated thermogenic gas seems to be a favorable interpretation for the hydrocarbon gas in the L1 gas pool thus far.

Hydrogen isotopes were first introduced in this study to better recognize the genetic types of the hydrocarbon gas in the L1 gas pool. According to the cross-plots of δ^{13}C-CH_4 vs. δD-CH_4 (Fig. 6), the gas samples from the L1 gas pool are most likely to be oil- to condensate-associated thermogenic gas with great possible microbial gas mixing. The genetic diagram advocated by Schoell (1983), in particular, highlights the possible mixed gases (Fig. 6a). Although the diagrams of Whiticar (1999, 2020) and Milkov and Etiope (2018) both indicate oil-associated thermogenic gas, the possibility of microbial gas mixing has also been highlighted (Figs 6b and c). The hydrogen isotopes of methane are suggested to be controlled by three major factors: hydrogen isotopic composition of kerogens in source rocks, thermal maturity, and ancient water medium during gas formation (Liu et al., 2019). Under the circumstance of similar maturity, marine source rocks generally produce D-enriched methane, while methane produced from source rocks in terrestrial freshwater settings is relatively depleted in D (Wang et al., 2015; Liu et al., 2019). The δD-C_1 value of –190‰ is declared to distinguish marine from terrigenous facies; however, this classification scheme should be used with caution because of the complex chemical reactions of hydrogen atoms during methane generation (Liu et al., 2019).

The models advocated by Milkov and Etiope (2018) did not take the gases of specific origins (humic-type or sapropelic-type) into consideration; therefore, new approaches recently developed by Milkov (2021) were employed in this study. According to the plot of $\delta^{13}C_1$ vs. $\delta^{13}C_2$ (Fig. 7a), the gas samples of the L1 gas pool was plotted at the sapropelic/humic separation line within the oil-associated thermogenic gas region. The diagram of $\delta^{13}C_1$ vs. $\Delta(\delta^{13}C_2–\delta^{13}C_1)$ also demonstrates an oil-associated ther-

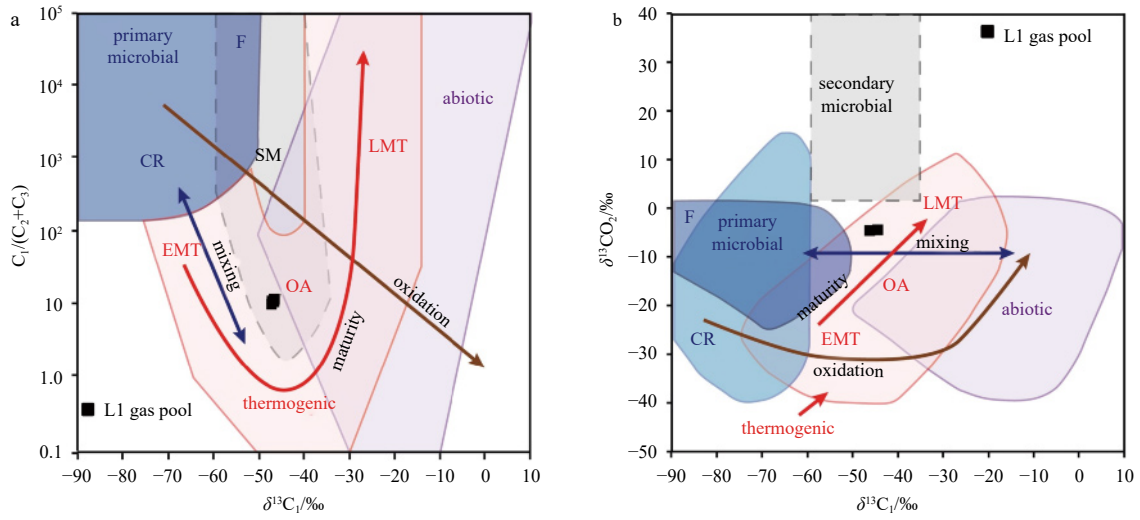

Fig. 5. Natural gases from the L1 gas pool plotted on genetic diagrams (modified after Milkov and Etiope (2018)). a. $C_1/(C_2+C_3)$ vs. $\delta^{13}C_1$ diagram; b. $\delta^{13}C_1$ vs. $\delta^{13}CO_2$ diagram. CR, CO_2 reduction; EMT, early mature thermogenic gas; F, methyl-type fermentation; LMT, late mature thermogenic gas; OA, oil-associated thermogenic gas; SM, secondary microbial.

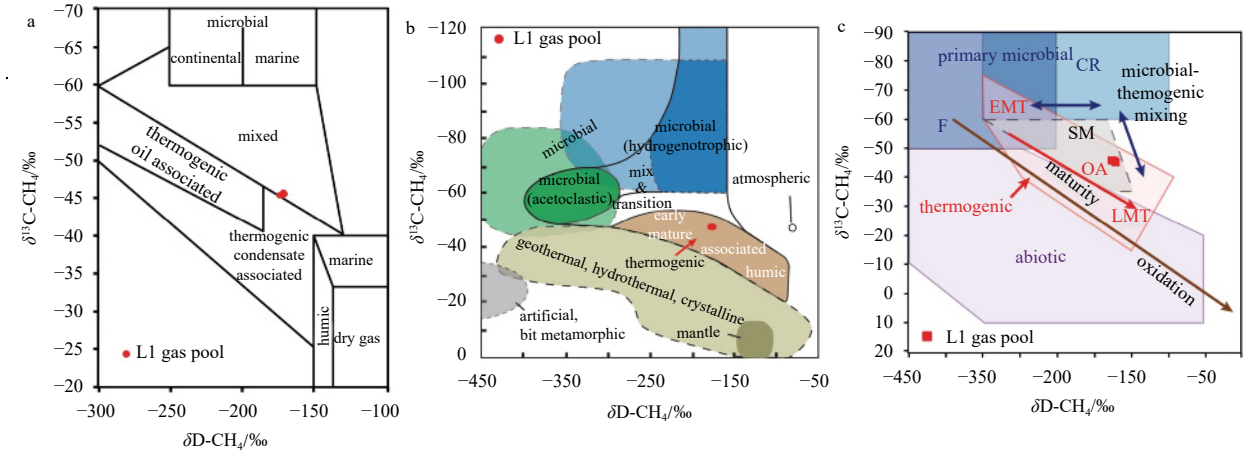

Fig. 6. Natural gases of the L1 gas pool plotted on methane genetic diagrams of δ^{13}C-CH_4 vs. δD-CH_4. a. modified after Schoell (1983); b. modified after Whiticar (1999, 2020); c. modified after Milkov and Etiope (2018). CR, CO_2 reduction; EMT, early mature thermogenic gas; F, methyl-type fermentation; LMT, late mature thermogenic gas; OA, oil-associated thermogenic gas; SM, secondary microbial.

mogenic gas and is unable to distinguish whether the gas is a sapropelic-type or humic-type gas (Fig. 7b). Despite the uncertainty of sapropelic-type or humic-type gas, the diagram of $\delta^{13}C_1$ vs. $\Delta(\delta^{13}C_2-\delta^{13}C_1)$ provides a compelling clue for a mixed microbial and thermogenic gas for the hydrocarbon gas in the L1 gas pool (Fig. 7b). As discussed previously, the hypothesis of secondary microbial gas does not work out for the hydrocarbon gas of the L1 gas pool due to the absence of biodegradation traces.

To further validate the findings of possible microbial gas mixing with oil-associated thermogenic gas in the L1 gas pool, cross-plots of $\delta^{13}C_1$ vs. $\delta^{13}C_2$ and $\delta^{13}C_2$ vs. $\delta^{13}C_3$ from Berner and Faber (1996) are utilized. Figure 8 illustrates the empirical trendlines for the carbon isotopic compositions in gas compounds at different levels of thermal maturity. According to the cross-plot of $\delta^{13}C_2$ vs. $\delta^{13}C_3$ (Fig. 8a), the perfect fitting of the L1 gas samples into the model implies that those gases are probably sourced from type II kerogens (sapropelic kerogen-sourced) in the late oil-window stage (R_o≈1.1%). C_2H_6 and C_3H_8 gases are both most likely to share the same thermal maturity and origin. The cross-plot of $\delta^{13}C_1$ vs. $\delta^{13}C_2$, on the contrary, suggests a seemingly abnormal pattern with an evident negative shift of $\delta^{13}C_1$ (Fig. 8b). As shown in Fig. 8b, if $\delta^{13}C_1$ values were adjusted toward the treadline in a ^{13}C enriched direction while $\delta^{13}C_2$ values remained constant, R_o would be approximately 1.1%, which perfectly matches the result in the cross-plot of $\delta^{13}C_2$ vs. $\delta^{13}C_3$. As microbial gas is typically characterized by a large CH_4 content as well as a significantly enriched $^{12}C_1$, this negative shift of $\delta^{13}C_1$ without the involvement of $\delta^{13}C_2$ and $\delta^{13}C_3$ considerably supports the hypothesis of mixed thermogenic and microbial gases in the L1 gas pool. The pure thermogenic CH_4 in the L1 gas pool is estimated to have $\delta^{13}C$ values of approximately –39.5‰ accordingly (Fig. 8b). Although the genetic diagrams of Berner and Faber (1996) were criticized by Milkov (2021) to inadequately infer sources of natural gases, they provide invaluable insights into the gas interpretations of the L1 gas pool.

When $\delta^{13}C$ values of methane through butane (C_1–C_4) from the L1 gas pool is plotted on the natural gas plot (Fig. 9), a lack of a linear or semilinear feature of the profile provides a strong indication for the gas mixing (Chung et al., 1988; Milkov et al., 2007; Milkov, 2021). Based on the methodology defined by Chung et al. (1988), the pure thermogenic CH_4 is estimated to have $\delta^{13}C$ values of approximately –38.5‰, which is consistent with the estimation derived from the aforementioned models declared by Berner and Faber (1996). Moreover, the mixing model would also aid

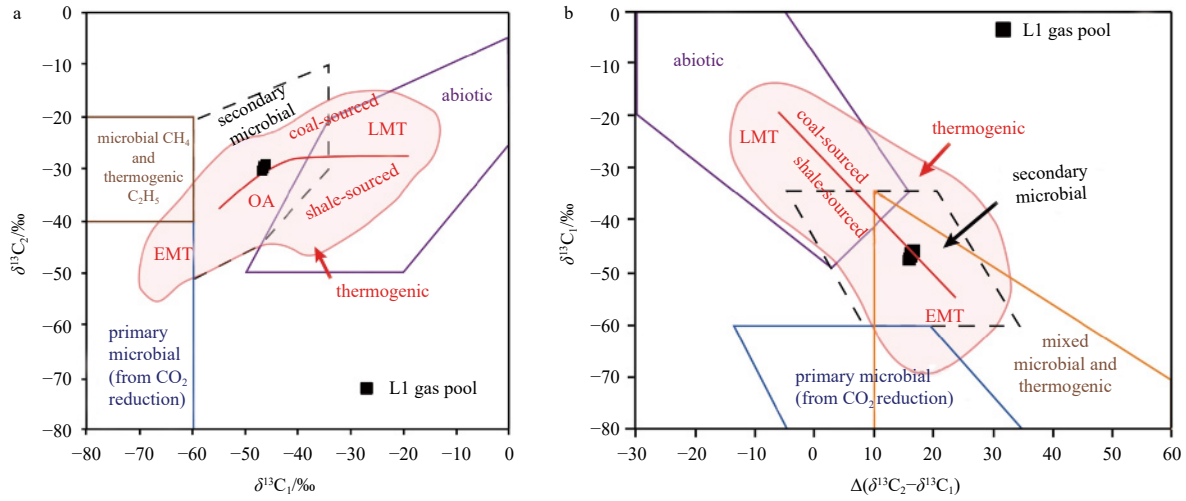

Fig. 7. Natural gases of the L1 gas pool plotted on genetic diagrams (modified after Milkov, 2021). a. $\delta^{13}C_1$ vs. $\delta^{13}C_2$ and b. $\delta^{13}C_1$ vs. $\Delta(\delta^{13}C_2-\delta^{13}C_1)$. EMT, early mature thermogenic gas; LMT, late mature thermogenic gas; OA, oil-associated thermogenic gas.

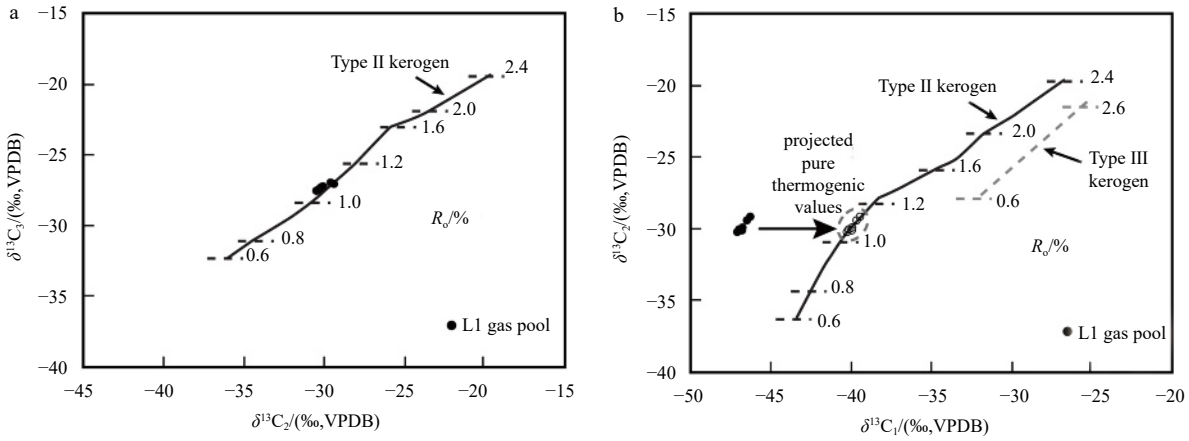

Fig. 8. Natural gases of the L1 gas pool plotted on genetic diagrams (modified after Berner and Faber, 1996). a. $\delta^{13}C_2$ vs. $\delta^{13}C_3$, b. $\delta^{13}C_1$ vs. $\delta^{13}C_2$. The carbon isotope values of the pure thermogenic gas are inferred by the parallel shifts of $\delta^{13}C_2$ values to the treadline. R_o, vitrinite reflectance.

in solving the debate between the oil-associated gas interpreted from the lighter $\delta^{13}C$ values of CH_4 and the wet-gas signature reflected by a relatively high GOR value of 5 764 m^3/m^3 (9 252 m^3/m^3 if CO_2 is counted) declared by Sun and Xi (2003) and Chen et al. (2008). Given the fact that a mixed gas is suggested for the hydrocarbon gas of the L1 gas pool, it is critical to assess each contribution of microbial and thermogenic gases. Unfortunately, the carbon isotope value of pure microbial methane has never been retrieved in the ECSSB. A presumably average $\delta^{13}C$ value of –70.00% is thereby assigned to the pure microbial methane according to the well-established microbial gas dataset compiled by Schoell (1983), Chung et al. (1988), and Katz (2011). The average stable carbon isotope value of methane in the L1 gas pool is inferred to be –46.54‰ from this paper. According to the unmixing calculation (Chung et al., 1988) of microbial methane ($\delta^{13}C_1$=–70.00‰) and thermogenic methane ($\delta^{13}C_1$=–39.00‰) as end-members, the pure microbial methane would account for ~24% of the total methane.

Overall, the natural gases of the L1 gas pool are estimated to comprise approximately 13% microbial methane ($\delta^{13}C_1$≈–70.00‰), approximately 48% mid-maturity sapropelic-type gas ($\delta^{13}C_1$≈ –39.00‰, $\delta^{13}C_2$≈–29.95‰, $\delta^{13}C_3$≈–27.36‰, $\delta^{13}n\ C_4$≈–26.72‰), and 39% of nonhydrocarbon gas (CO_2 and N_2). This model was further validated by comparing the outcomes of the gold tube thermal simulation experiments conducted by Chen et al. (2008). The measurements were conducted by using 10–40 mg kerogens

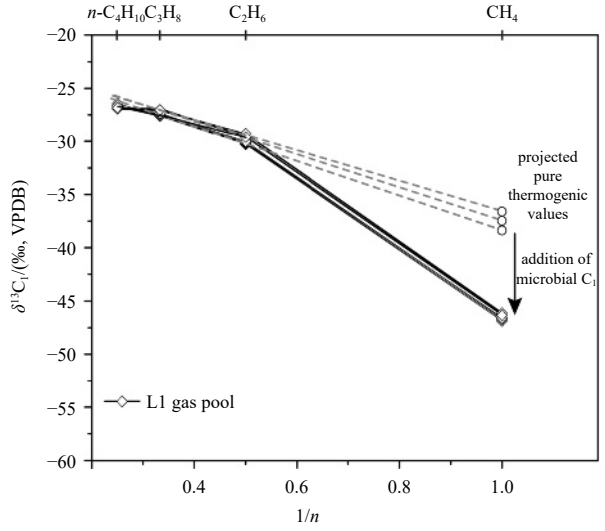

Fig. 9. Carbon isotopic compositions of C_1–C_4 gases from the L1 gas pool exhibited on the natural gas plot (Chung et al., 1988). Dashed lines indicate the extrapolation of carbon isotope values of C_2–C_4 gases to obtain the estimated $\delta^{13}C$ of pure thermogenic methane from –37.0‰ to –38.5‰.

in a gold tube autoclave under a constant pressure of 50 MPa and temperatures from 150℃ to 425/450℃ at a rate of 20℃/h. It is worth noting that one of the best source rock samples (high HI and TOC values) in the Lishui-Jiaojiang Sag was collected in their study (Table 6; Fig. 1). This unique sample was also one of the few available immature Yueguifeng source rocks for the gold tube pyrolysis measurements. According to Chen et al. (2008), the gases from the Yueguifeng Formation at the early mature stage (i.e., the Yueguifeng sample from Well W1 with a temperature of 425℃) attained $\delta^{13}C_1$, $\delta^{13}C_2$, and $\delta^{13}C_3$ values of ~–37‰, ~–30‰, and ~–29‰, respectively (Table 6). As the maturity evolved to the peak mature stage (i.e., the Yueguifeng sample from Well W1 with a temperature of 450℃ and the Yueguifeng sample from Well W2 with R_o=1.07% in Table 6), the gases would obtain $\delta^{13}C_1$ values in the rage of –37‰ to –42‰, which were declared to closely resemble the scenario of the L1 gas pool by taking an extra isotopic fractionation of ~3‰ into consideration (Chen et al., 2008). However, their conclusions were not unequivocal without elucidating the occurrence of a more ^{13}C-depleted CH_4 but considerably ^{13}C-enriched C_2H_6/C_3H_8 from a "peak maturity source rock" (Table 6). In addition, only the results of immature samples with relatively high HI values (samples from Well W1) are valid due to the strict sampling criteria for the thermal simulation measurements. The same sampling issue also happened to Li et al. (2021) as their samples have low HI values and relatively high maturities. Nevertheless, the average carbon isotopic fingerprints of the pyrolysis gas of two Yueguifeng mudstones from Well W1 ($\delta^{13}C_1$=–37.45‰, $\delta^{13}C_2$=–30.63‰, $\delta^{13}C_3$=–28.22‰, $\delta^{13}nC_4$=–25.37‰) bear close resemblance to the calculated pure thermogenic gas in the L1 gas field ($\delta^{13}C_1$≈–39.00‰, $\delta^{13}C_2$≈ –29.95‰, $\delta^{13}C_3$≈–27.36‰, $\delta^{13}n\ C_4$≈–26.72‰), delivering additional compelling evidence for the proposed mixed gas model. The author acknowledges that the gold-tube pyrolysis by Chen et al. (2008) simulated an anhydrous closed system, and their experiment may not reflect actual subsurface conditions such as temperature, pressure, presence of water and minerals, and migrations. The actual evolution of the carbon isotopic compositions of the hydrocarbon gases in the reservoir may also show complex long-term cumulative patterns (e.g., Tang et al., 2000). Therefore, additional gold-tube pyrolysis of appropriate source rocks and molecular and isotopic measurements of hydrocarbons in the Lishui-Jiaojiang Sag are required in a future study to further attest to the mixed gas model of the L1 gas field. It is important to emphasize that careful consideration should be given to the $\delta^{13}C_1$ vs. R_o relationships due to the complex geologic processes (e.g., migration, charging, mixing, and degradation). The imprudent applications of various empirical $\delta^{13}C_1$-R_o regression equations into the gas interpretation in the previous studies have notably misled the identification of L1 gas source rocks (e.g., Su et al., 2014, Li et al., 2021).

Table 6. Selected geochemical parameters of source rock samples and carbon isotopic compositions of thermal simulation products (modified after Chen et al., 2008).

Well	Formation	Source rock assessment				Simulation	Yield rate of hydrocarbons/	C isotopes of simulated gas/‰					Data source
		TOC/%	R_o/%	HI/(mg·g^{-1})	$\delta^{13}C$/‰	T/℃	(mL·g^{-1})	C_1	C_2	C_3	i-C_4	n-C_4	
W1	YGF	2.65	0.58	344	–26.3	425	98.67	–37.96	–30.92	–29.61	–29.23	–27.95	Chen et al. (2008)
	YGF	2.65	0.58	344	–26.3	450	146.64	–36.95	–30.33	–26.83	–26.09	–22.78	
W2	YGF	2.89	1.07	74	–28.1	450	43.01	–42.18	–23.39	–17.71	–	–	
	LF	1.61	0.88	80	–26.4	450	66.07	–31.43	–19.97	–12.98	–	–	
L1	LF	0.85	0.8	69	–25.3	450	64.47	–33.06	–21.04	–15.28	–	–	

Note: YGF, Yueguifeng; LF, Lingfeng. See Fig. 1b for well locations.

5.2 *Origin of the condensate oils in the L1 gas pool*

Light hydrocarbons have been commonly used for assessing oil types, maturations, and other characteristics (Thompson, 1983, 1987; Dai et al., 1992; Ten Haven, 1996; Mango, 1997; Hu et al., 2008, 2017). The ternary plot of relative contents of C_7 light hydrocarbons (including MCH, *n*-C_7, DMCP) has been proposed to be useful in interpreting the source rocks of hydrocarbons (Dai et al., 1992; Hu et al., 2008). MCH, which is predominantly derived from terrestrial higher plants, dominates the C_7 light hydrocarbons in the L1 oil samples (Fig. 10). Therefore, the L1 oil samples are most likely to be sourced from humic kerogen-rich source rocks. Such an origin is also supported by the average pristane (Pr) to phytane (Ph) ratio Pr/Ph≈5.0 of the oil discovered in the L1 gas field (Sun and Xi, 2003; Ge et al., 2012).

The cross-plots of *iso*-heptane values vs. *n*-heptane values and *n*-heptane/methylcyclohexane vs. toluene/*n*-heptane proposed by Thompson (1983, 1987) are introduced in this study, to better understand the maturity, source rocks, and processes of the condensate accumulations. In the cross-plots of *iso*-heptane values vs. *n*-heptane values, the L1 oil samples are mainly plotted in the normal to mature oil regions as well as the Type-III kerogen rich curve (Fig. 11a). The separations of *iso*-heptane values between production wells and discovery well in Fig. 11a are most likely due to the different sampling processes, but debates still exist. The *n*-heptane/methylcyclohexane values (paraffinicity) of all samples are in the range of 0.31–0.34, whereas toluene/*n*-heptane values (aromaticity) for most samples are between 0.39 and 0.51. Based on the paraffinicity and aromaticity relationships (Fig. 11b), the L1 condensate oil samples are generally interpreted to be normal oil. A relatively short migration distance is thereby inferred. However, care should be taken by applying the cross-plot of *n*-heptane/methylcyclohexane vs. toluene/*n*-heptane as the dataset is extremely limited, and deeper oil samples are in need to disentangle this uncertainty. The saturated hydrocarbon enriched L1 oil contains a full range of *n*-alkanes (Fig. 3, Table 4), suggesting a lack of major biodegradation. It is also worth noting that gasoline-range hydrocarbons have significantly low abundances of benzene but high abundances of cyclohexane and methylcyclohexane (Fig. 3), which may be linked to the distinct kerogen sources. The ratio of 2, 4-dimethylpentane and 2, 3-dimethylpentane (2, 4-DMP/2, 3-DMP) from light hydrocarbons has been calibrated as a proxy for the temperature of hydrocarbon generation (Mango, 1987, 1990, 1997). The relationship was published by BeMent et al. (1995) as follows: $T(℃)$= 140+15(ln[2, 4-DMP)/2, 3-DMP]). According to their equations, the hydrocarbon-generating temperatures of L1 oil samples were calculated to be in the range of 126.5℃ to 127.2℃, with an average value of 126.9℃. The results are consistent with the aforementioned interpretation of the Lingfeng-sourced oil as the corresponding oil generation temperatures range between ~120℃ and ~140℃ (discussed in Section 5.3).

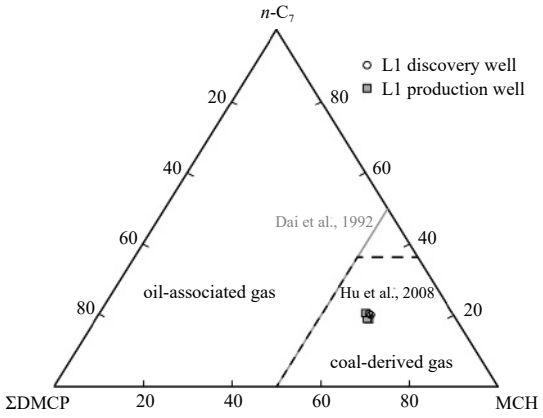

Fig. 10. Ternary plot showing the distribution of C_7 light hydrocarbons in condensate oil samples of the L1 gas pool (modified after Dai et al., 1992; Hu et al., 2008).

5.3 *Petroleum accumulation history of the L1 gas pool*

According to this study, the hydrocarbon fluids in the L1 gas field are apparently from different source rocks. The hydrocarbon gases in the L1 gas pool are interpreted to be mixed thermogenic and microbial gases, in which the pure thermogenic gas is from sapropelic kerogen-rich source rocks (i.e., the Yueguifeng Formation) in the late oil-window stage (R_o≈1.1%), and the microbial methane was interpreted to be from the immature Mingyuefeng Formation *in situ*. The L1 oil is most likely to be normal oil (R_o≈0.9%) and derived from humic kerogen-rich source rocks.

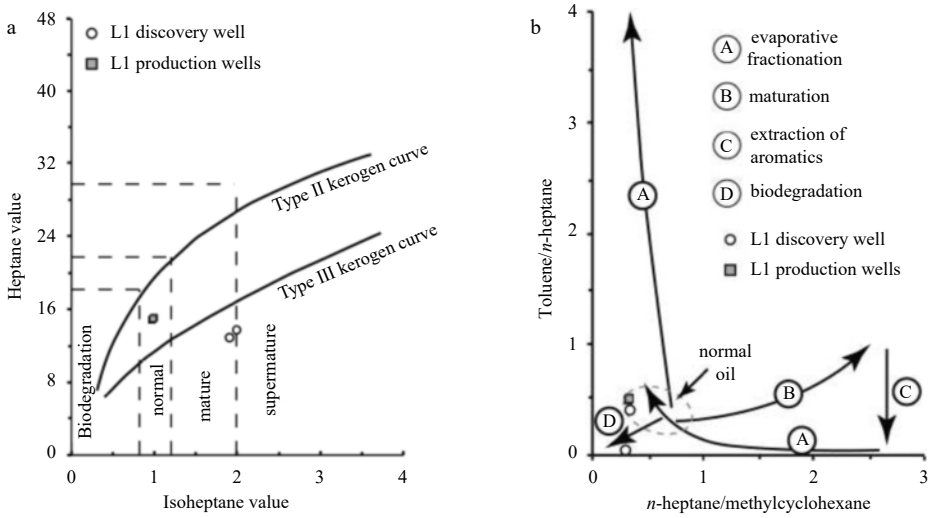

Fig. 11. Condensate oil samples from the L1 gas pool plotted on the two commonly used diagrams for light hydrocarbon interpretations. a. Cross-plot of *n*-heptane values vs. *iso*-heptane values (modified after Thompson, 1983), and b. cross-plot of *n*-heptane/methylcyclohexane vs. toluene/*n*-heptane (modified after Thompson, 1987).

The base of the Mingyuefeng Formation is typically immature except that a small portion adjacent to the Lingfeng Uplift has reached the early mature stage with a maximum Ro of ~0.8%. The thermogenic oil in the L1 gas field is thus most likely to be charged from deeper buried Lingfeng Formation. Combining burial-thermal histories (Fig. 12), the generation of the oil-associated sapropelic-type gas (R_o≈1.0%–1.3%) from the Yueguifeng Formation most likely occurred during 52–41 Ma. The humic kerogen-rich Lingfeng Formation entered the oil window at approximately 52 Ma and had remained in the mid-maturity stage (corresponding formation temperatures of approximately 120–140℃) prior to the late Eocene–Oligocene uplift (Fig. 12). Since the late Eocene, further thermal decomposition of both source rocks had significantly decelerated as they had never reached the maximum burial depth again (Fig. 12). Considering all factors of the elevated GOR value, apparently different maturities between thermogenic gas and oil, and one gas charging stage, a small amount of oil from the Lingfeng Formation was most likely dissolved along with the gas migration from the Yueguifeng Formation and then eventually reached the L1 trap during the late Eocene–Oligocene.

The key factor controlling the development of microbial gas is the temperature (Katz, 2011). Microbial gas is classified into two categories primary and secondary, and the former is formed by microbes from organic matter in a relatively shallow, cool, and anoxic environment (temperatures<80℃, optimal temperature <60℃) (Katz, 2011). This kind of gas is commonly derived from CO_2 reduction and acetic acid fermentation (Whiticar, 1996, 2020; Katz, 2011; Milkov and Etiope, 2018). Secondary microbial gas is produced from petroleum biodegradation by the microbes (Katz, 2011; Milkov and Etiope, 2018). In the case of the L1 gas field, the model of the primary microbial gas is proposed since no evidence of secondary microbial methane (i.e., oil biodegradation) has been reported in this study. The current reservoir is buried at ~85℃ and a depth of ~2 200 m TVDSS. Therefore, shallower depths and lower temperature conditions in the geologic past are indicated for the formation of microbial gas. According to the burial-thermal history model of the Well L1 (Fig. 12), the generation of primary microbial gases would be no later than the middle Eocene by adopting the temperature of 80℃ tolerated by microbes. The reservoir depth was generally less than 1 600 m. The primary microbial gases were subsequently trapped in the Mingyuefeng Formation along with the rapid burial. It is worth noting that although the temperature of the Mingyuefeng reservoir fell below 60℃ during the Miocene due to the substantial late Eocene-Oligocene uplift (Fig. 12), the microbes would have been eliminated during the late Eocene as temperatures exceeded 80℃ (Katz, 2011).

The misinterpretations of oil and gas in the L1 gas field by using empirical geochemical approaches in all previous studies had considerably hindered a clear understanding of the Paleocene petroleum system. This study, discerning the origins of hydrocarbons and their charge history in the L1 gas field, has significant geological implications for regional hydrocarbon explorations. The possible shallow accumulation or mixing of varying amounts of microbial gas should be taken into account, in particular to the thermally immature humic-kerogen-rich Mingyuefeng Formation. The author has proposed that approximately 24% of total methane in the L1 gas pool may have microbial origin. Despite the fact that the microbial gas is less quantitatively significant than the thermogenic gas, it still suggests the volumetric and economic significance of microbial gas in the Lishui-Jiaojiang Sag, and even the other parts of the ECSSB. Regarding the thermogenic gas, the Yueguifeng mudstone is considered to be the principal source rock for the Paleocene petroleum system in the Lishui-Jiaojiang Sag. Therefore, an assessment of the spatial distribution of thermally mature and organic-rich Yueguifeng source rock is of great importance to the hydrocarbon exploration in the Lishui-Jiaojiang Sag.

6 Conclusions

The integrated study of the genetic molecular compositions,

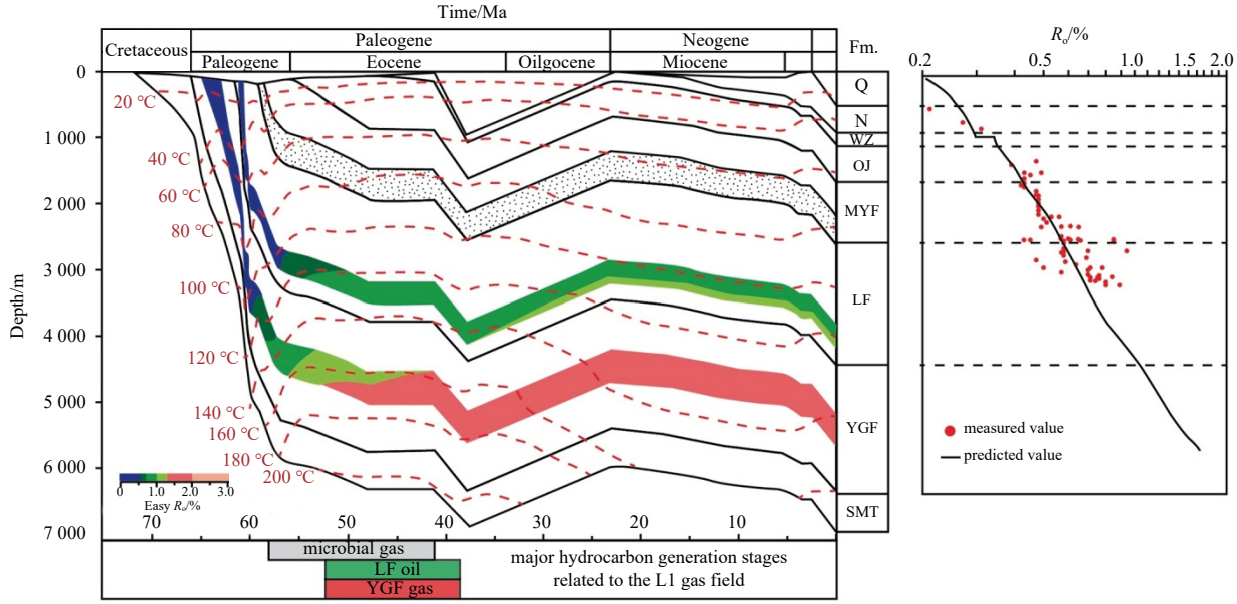

Fig. 12. Schematic burial-thermal histories reconstructed for the Well L1 by the 1D model of PetroMod software. Thermal evolutions and major hydrocarbon generation histories of both Yueguifeng and Lingfeng source rocks have been highlighted. Easy R_o is calculated after Sweeney and Burnham (1990). MYF, Mingyuefeng; LF, Lingfeng.; YGF, Yueguifeng; SMT, Shimentan; OJ, Oujiang; WZ, Wenzhou; N, Neogene; Q, Quaternary; Fm., formation.

carbon and hydrogen isotopes, and light hydrocarbon signatures of the hydrocarbon fluids in the L1 gas field has established a significant breakthrough in the hydrocarbon accumulation model of the Lishui-Jiaojiang Sag, East China Sea Shelf Basin. The mixing model of the L1 gas field suggests a continuum of processes that varied correspondingly to the source rocks, maturation, migration, mixing, and other controlling factors. This study establishes a protocol for recognizing the microbial gases and would aid in further exploration strategies by providing significant insights into the genetic characterizations of hydrocarbon fluids in the East China Sea Shelf Basin.

(1) The hydrocarbon gas, accounting for approximately 61% of the natural gases of the L1 gas pool, was quantified to comprise approximately 24% microbial methane from the Mingyuefeng Formation *in situ*, and approximately 76% sapropelic-type thermogenic gas from the Yueguifeng Formation. This is in great contrast to the long-held belief of the pure thermogenic gas in all previous studies.

(2) The oils in the L1 gas pool were interpreted to be mid-mature (R_o≈0.9%) and sourced from humic kerogen-rich source rocks of the Lingfeng Formation. The sapropelic-type thermogenic gas in the L1 gas pool is interpreted to be in the late oil-window stage (R_o≈1.1%). The small amount of oil from the Lingfeng Formation is most likely to be picked up by the migrating gas from the Yueguifeng Formation during the middle to late Eocene.

(3) The author would warn against assigning thermogenic gas instinctively even if there exist enriched $^{13}C_1$ ($\delta^{13}C_1$>−50‰) and $C_1/\Sigma(C_1–C_5)$ < 95% in the natural gas. It is prudent to acknowledge that all genetic diagrams for gas interpretation should be applied with care as most of them are empirical and may not be globally applicable. Care should also be taken when establishing or applying various relationships between carbon/hydrogen isotopes and other geologic parameters (e.g., R_o) without a clear understanding of the gas types. Therefore, an integrated approach should be utilized to understand the complex processes and variability of elements in the petroleum system.

Acknowledgement

The author thanks the Shanghai Branch of China National Offshore Oil Corporation (CNOOC) Co., Ltd. for permission to publish.

References

BeMent W O, Levey R A, Mango F D. 1995. The temperature of oil generation as defined with C_7 chemistry maturity parameter (2, 4-DMP/2, 3-DMP ratio). In: Grimalt J O, Dorronsoro C, eds. Organic Geochemistry: Developments and Applications to Energy, Climate, Environment and Human History. Donostian-San Sebastian: European Association of Organic Geochemists, 505–507

Bernard B B, Brooks J M, Sackett W M. 1976. Natural gas seepage in the Gulf of Mexico. Earth and Planetary Science Letters, 31(1): 48–54, doi: 10.1016/0012-821X(76)90095-9

Berner U, Faber E. 1996. Empirical carbon isotope/maturity relationships for gases from algal kerogens and terrigenous organic matter, based on dry, open-system pyrolysis. Organic Geochemistry, 24(10/11): 947–955

Cesar J, Nightingale M, Becker V, et al. 2020. Stable carbon isotope systematics of methane, ethane and propane from low-permeability hydrocarbon reservoirs. Chemical Geology, 558: 119907, doi: 10.1016/j.chemgeo.2020.119907

Chen Jianping, Ge Heping, Chen Xiaodong, et al. 2008. Classification and origin of natural gases from Lishui Sag, the East China Sea Basin. Science in China Series D: Earth Sciences, 51(1): 122–130

Chung H M, Gormly J R, Squires R M. 1988. Origin of gaseous hydrocarbons in subsurface environments: theoretical considerations of carbon isotope distribution. Chemical Geology, 71(1–3): 97–104

Cukur D, Horozal S, Kim D C, et al. 2011. Seismic stratigraphy and structural analysis of the northern East China Sea Shelf Basin interpreted from multi-channel seismic reflection data and cross-section restoration. Marine and Petroleum Geology, 28(5): 1003–1022, doi: 10.1016/j.marpetgeo.2011.01.002

Dai Jinxing, Gong Deyu, Ni Yunyan, et al. 2014. Stable carbon isotopes of coal-derived gases sourced from the Mesozoic coal measures in China. Organic Geochemistry, 74: 123–142, doi: 10.1016/j.orggeochem.2014.04.002

Dai Jinxing, Pei Xigu, Qi Houfa. 1992. Natural Gas Geology in China, vol. 1 (in Chinese). Beijing: Petroleum Industry Press, 35–86

Ge Heping, Chen Xiaodong, Diao Hui, et al. 2012. An analysis of oil geochemistry and sources in Lishui sag, East China Sea basin. China Offshore Oil and Gas (in Chinese), 24(4): 8–12,31

Hu Guoyi, Li Jian, Li Jin, et al. 2008. Preliminary study on the origin identification of natural gas by the parameters of light hydrocarbon. Science in China Series D: Earth Sciences, 51(S1): 131–139, doi: 10.1007/s11430-008-5017-x

Hu Guoyi, Peng Weilong, Yu Cong. 2017. Insight into the C_8 light hydrocarbon compositional differences between coal-derived and oil-associated gases. Journal of Natural Gas Geoscience, 2(3): 157–163, doi: 10.1016/j.jnggs.2017.08.001

Huang Yaohao, Tarantola A, Lu Wanjun, et al. 2020. CH_4 accumulation characteristics and relationship with deep CO_2 fluid in Lishui sag, East China Sea Basin. Applied Geochemistry, 115: 104563, doi: 10.1016/j.apgeochem.2020.104563

Katz B J. 2011. Microbial processes and natural gas accumulations. The Open Geology Journal, 5: 75–83, doi: 10.2174/1874262901105010075

Li Deyong, Dong Bingjie, Jiang Xiaodian, et al. 2016. Geochemical evidence for provenance and tectonic background from the Palaeogene sedimentary rocks of the East China Sea Shelf Basin. Geological Journal, 51(S1): 209–228

Li Yang, Zhang Jinliang, Liu Yang, et al. 2019. Organic geochemistry, distribution and hydrocarbon potential of source rocks in the Paleocene, Lishui Sag, East China Sea Shelf Basin. Marine and Petroleum Geology, 107: 382–396, doi: 10.1016/j.marpetgeo.2019.05.025

Li Yang, Zhang Jinliang, Xu Yaohui, et al. 2021. Improved understanding of the origin and accumulation of hydrocarbons from multiple source rocks in the Lishui Sag: Insights from statistical methods, gold tube pyrolysis and basin modeling. Marine and Petroleum Geology, 134: 105361, doi: 10.1016/j.marpetgeo.2021.105361

Liang Jintong, Wang Hongliang. 2019. Cenozoic tectonic evolution of the East China Sea Shelf Basin and its coupling relationships with the Pacific Plate subduction. Journal of Asian Earth Sciences, 171: 376–387, doi: 10.1016/j.jseaes.2018.08.030

Liu Quanyou, Wu Xiaoqi, Wang Xiaofeng, et al. 2019. Carbon and hydrogen isotopes of methane, ethane, and propane: A review of genetic identification of natural gas. Earth-Science Reviews, 190: 247–272, doi: 10.1016/j.earscirev.2018.11.017

Mango F D. 1987. An invariance in the isoheptanes of petroleum. Science, 237(4814): 514–517, doi: 10.1126/science.237.4814.514

Mango F D. 1990. The origin of light hydrocarbons in petroleum: a kinetic test of the steady-state catalytic hypothesis. Geochimica et Cosmochimica Acta, 54(5): 1315–1323, doi: 10.1016/0016-7037(90)90156-F

Mango F D. 1997. The light hydrocarbons in petroleum: a critical review. Organic Geochemistry, 26(7–8): 417–440

Milkov A V, Dzou, L. 2007. Geochemical evidence of secondary microbial methane from very slight biodegradation of undersaturated oils in a deep hot reservoir. Geology, 35(5): 455–458, doi: 10.1130/G23557A.1

Milkov A V. 2021. New approaches to distinguish shale-sourced and coal-sourced gases in petroleum systems. Organic Geochemistry, 158: 104271, doi: 10.1016/j.orggeochem.2021.104271

Milkov A V, Etiope G. 2018. Revised genetic diagrams for natural

gases based on a global dataset of >20, 000 samples. Organic Geochemistry, 125: 109–120, doi: 10.1016/j.orggeochem.2018.09.002

Schellart W P, Lister G S. 2005. The role of the East Asian active margin in widespread extensional and strike-slip deformation in East Asia. Journal of the Geological Society, 162(6): 959–972, doi: 10.1144/0016-764904-112

Schoell M. 1980. The hydrogen and carbon isotopic composition of methane from natural gases of various origins. Geochimica et Cosmochimica Acta, 44(5): 649–661, doi: 10.1016/0016-7037(80)90155-6

Schoell M. 1983. Genetic characterization of natural gases. AAPG Bulletin, 67(12): 2225–2238

Su Ao, Chen Honghan, Cao Laisheng, et al. 2014. Genesis, source and charging of oil and gas in Lishui Sag, East China Sea Basin. Petroleum Exploration and Development, 41(5): 574–584, doi: 10.1016/S1876-3804(14)60068-9

Sun Yumei, Xi Xiaoying. 2003. Petroleum reservoir filling history and oil-source correlation in the Lishui Sag, East China Sea Basin. Petroleum Exploration and Development, 30(6): 24–28

Sweeney J J, Burnham A K. 1990. Evaluation of a simple model of vitrinite reflectance based on chemical kinectics. AAPG Bulletin, 74(10): 1559–1570

Tang Y, Perry J K, Jenden P D, et al. 2000. Mathematical modeling of stable carbon isotope ratios in natural gases. Geochimica et Cosmochimica Acta, 64(15): 2673–2687, doi: 10.1016/S0016-7037(00)00377-X

Ten Haven H L. 1996. Applications and limitations of Mango's light hydrocarbon parameters in petroleum correlation studies. Organic Geochemistry, 24(10/11): 957–976

Thompson K F M. 1983. Classification and thermal history of petroleum based on light hydrocarbons. Geochimica et Cosmochimica Acta, 47(2): 303–316, doi: 10.1016/0016-7037(83)90143-6

Thompson K F M. 1987. Fractionated aromatic petroleums and the generation of gas-condensates. Organic Geochemistry, 11(6): 573–590, doi: 10.1016/0146-6380(87)90011-8

Vandré C, Cramer B, Gerling P, et al. 2007. Natural gas formation in the western Nile delta (Eastern Mediterranean): Thermogenic versus microbial. Organic Geochemistry, 38(4): 523–539, doi: 10.1016/j.orggeochem.2006.12.006

Wang Xiaofeng, Liu Wenhui, Shi Baoguang, et al. 2015. Hydrogen isotope characteristics of thermogenic methane in Chinese sedimentary basins. Organic Geochemistry, 83–84: 178–189

Whiticar M J. 1996. Isotope tracking of microbial methane formation and oxidation. Internationale Vereinigung für Theoretische und Angewandte Limnologie: Mitteilungen, 25(1): 39–54

Whiticar M J. 1999. Carbon and hydrogen isotope systematics of bacterial formation and oxidation of methane. Chemical Geology, 161(1–3): 291–314

Whiticar M J. 2020. The biogeochemical methane cycle. In: Wilkes H, ed. Hydrocarbons, Oils and Lipids: Diversity, Origin, Chemistry and Fate. Springer, 669–746

Yang Shuchun, Hu Shengbiao, Cai Dongsheng, et al. 2004. Present-day heat flow, thermal history and tectonic subsidence of the East China Sea Basin. Marine and Petroleum Geology, 21(9): 1095–1105, doi: 10.1016/j.marpetgeo.2004.05.007